INTERNATIONAL JOURNAL FOR NUMERICAL METHODS IN FLUIDS
Int. J. Numer. Meth. Fluids 2005; **47**:1369–1374
Published online 12 January 2005 in Wiley InterScience (www.interscience.wiley.com). DOI: 10.1002/fld.897

Laboratory for internal gravity-wave dynamics: the numerical equivalent to the quasi-biennial oscillation (QBO) analogue

Nils P. Wedi[1,*,†] and Piotr K. Smolarkiewicz[2]

[1]*European Centre for Medium Range Weather Forecasts, Shinfield Park, RG2 9AX Reading, U.K.*
[2]*National Center for Atmospheric Research, Boulder, CO80307, U.S.A.*

SUMMARY

We have extended the classical terrain-following coordinate transformation of Gal–Chen and Somerville to a broad class of time-dependent vertical domains. The proposed extension facilitates modelling of undulating vertical boundaries in various areas of computational fluid dynamics. The theoretical development and the efficient numerical implementation have been documented in the context of the generic Eulerian/semi-Lagrangian, non-oscillatory forward in time (NFT), nonhydrostatic model framework. In particular, it allows the simulation of stratified flows with intricate geometric, time-dependent boundary forcings, either at the top or at the bottom of the domain. We have applied our modelling framework in the direct numerical simulation of the celebrated laboratory experiment of Plumb and McEwan creating the numerical equivalent to their quasi-biennial oscillation (QBO) analogue. The QBO represents a conspicuous example of a fundamental dynamical mechanism with challenging detail, which is difficult to deduce from experimental evidence alone. A series of 2D and 3D simulations demonstrate the ability to reproduce the laboratory results. The numerical experiments identify the developing periodically reversing mean flow pattern primarily as a wave–wave mean flow interaction-driven phenomenon. The results not only enhance the confidence in the numerical approach but further elevate the importance of the laboratory setup in its fundamental similarity to the atmosphere, while allowing the study of the principal atmospheric mechanisms and their numerical realizability in a confined 'laboratory' environment.

KEY WORDS: QBO; wave–wave and wave mean-flow interaction; generalized Gal–Chen and Somerville coordinate transformation; direct numerical simulation; tank experiments

1. INTRODUCTION

The quasi-biennial oscillation (QBO) represents the dominant variability in the equatorial stratosphere [1]. It exhibits a fundamental dynamical mechanism with challenging detail: the interaction of propagating waves with a mean flow. Holton and Lindzen [2, 3] were among

*Correspondence to: Nils P. Wedi, European Centre for Medium Range Weather Forecasts, Shinfield Park, RG2 9AX Reading, U.K.
†E-mail: wedi@ecmwf.int

Received 27 April 2004
Revised 6 December 2004
Accepted 6 December 2004

the first to present a conceptual model of the QBO describing this interaction. In a viscous, non-rotating[‡] Boussinesq fluid, the interaction can be described by the averaged momentum equations in a horizontally periodic domain as

$$\frac{\partial U}{\partial t} - \nu \frac{\partial^2 U}{\partial z^2} = -\sum_i \frac{\partial F_i}{\partial z} \tag{1}$$

where $U := \bar{u}^{xy}$ denotes the horizontally averaged (mean) flow, ν denotes the kinematic viscosity and $F := \overline{u'w'}^{xy}$ expresses the averaged nonlinear momentum flux.[§] Most atmospheric research of the QBO [1] is devoted to finding the precise physical origins of the rhs of Equation (1) and their numerical realizability in the context of numerical weather prediction and climate models. In spite of numerous studies, see Reference [1] for a recent review, a complete understanding of the QBO eludes the efforts.

The principal mechanism of the QBO was demonstrated in the laboratory experiment of Plumb and McEwan [5]. The laboratory analogue of the stratospheric equatorial oscillation consists of a cylindrical annulus filled with density-stratified salty water, forced at the lower boundary by an oscillating membrane. At sufficiently large forcing amplitude the wave motion generates a longer period zonal mean flow oscillation. The laboratory experiment is often employed to explain the basic mechanism of the atmospheric QBO [1]. However, it also has been criticized for its apparent fundamental difference to the QBO [6]. In the laboratory, the average momentum-flux convergence has been attributed almost exclusively to viscous and thermal dissipation of internal waves [5, 7, 8]. In the atmosphere, wave transience and subsequent breaking are considered chronologically more important primary causes of the zonal mean flow oscillation [6, 8]. Furthermore, it is argued that a continuous spectrum of waves, rather than a discrete pair of phase speeds, contributes to the QBO [8]. Consequently, a direct application of the analysis of the laboratory results to atmospheric observations has been questioned [6].

We employ a direct numerical simulation of the QBO analogue to resolve the apparent difference in interpretation. We demonstrate that our numerical model is able to reproduce the laboratory results while allowing a detailed analysis of the precise origin of the averaged momentum flux. We find that wave–wave mean flow interactions (see Reference [9] for a discussion) are the chronologically more important primary cause of the zonal mean zonal flow oscillation in the laboratory experiment—in analogy to the effect of wave transience in a compressible atmosphere [6]. It elevates the importance of the laboratory setup for its fundamental similarity to the atmosphere. This allows us to utilize the conceptual simplicity of the experiment to investigate various aspects of numerical realizability and parametric dependence of the atmospheric QBO in a well-observed confined 'laboratory' environment. Ultimately, it is our aim to provide a catalogue of sensitivities that can be employed in numerical weather prediction and climate models to enable the successful simulation of such a mean-flow oscillation.

[‡]The QBO has its maximum at the equator where the Coriolis parameter $f = 0$.

[§]In the context of time-varying mean flow oscillations it is important to note that the second 'Eliassen–Palm theorem' [4], stating the height independence of the vertical flux of horizontal momentum $\overline{u'w'}^{xy}$, refers to a steady state in the absence of damping and critical levels.

2. THE NUMERICAL MODEL

The equations of motion for a non-rotating, density-stratified viscous Boussinesq fluid—an appropriate approximation for salty water [10]—are

$$\begin{aligned} \nabla \cdot (\rho_0 \mathbf{v}) &= 0 \\ \frac{\mathrm{D}\mathbf{v}}{\mathrm{D}t} &= -\nabla \pi' + \mathbf{g}\frac{\rho'}{\rho_0} + \frac{1}{\rho_0}\nabla \cdot \tau \\ \frac{\mathrm{D}\rho'}{\mathrm{D}t} &= \kappa \nabla^2 \rho' - \mathbf{v} \cdot \nabla \rho_e \end{aligned} \tag{2}$$

Here, the operators $\mathrm{D}/\mathrm{D}t$, ∇, and $\nabla\cdot$ symbolize the material derivative, gradient, and divergence; $\mathbf{v}$ denotes the velocity vector; ρ' and π' denote, respectively, density and normalized-pressure perturbations with respect to the static ambient state characterized by the linearly stratified profile ρ_e; $\mathbf{g}$ symbolizes the gravity vector, and ρ_0 a constant reference density. $\nabla \cdot \tau$ is the divergence of the viscous stress tensor (a kinematic viscosity $\nu = 1.004 \times 10^{-6}\ \mathrm{m^2\ s^{-1}}$ is assumed); and $\kappa\,(= 1.5 \times 10^{-9}\ \mathrm{m^2\ s^{-1}})$ is the diffusivity of salt in water.

Equations (2) are cast in a time-dependent curvilinear framework [11, 12], employing the generalized Gal–Chen coordinate transformation

$$\bar{t} = t, \quad \bar{x} = x, \quad \bar{y} = y, \quad \bar{z} = H_0 \frac{z - z_s(x, y, t)}{H(x, y, t) - z_s(x, y, t)} \tag{3}$$

whose theoretical development and efficient numerical implementation were discussed thoroughly in Reference [13]. Transformation (3) allows for time-dependent upper, $H(x, y, t)$, and lower, $z_s(x, y, t)$, boundary forcings without small-amplitude approximations. In particular, it enables the direct numerical simulation of the laboratory experiment. In standard atmospheric models a major uncertainty arises from the lack of knowledge of the required wave forcing and its numerical realizability, rendering a detailed analysis of the QBO more difficult.

The governing equations (2) are integrated numerically in the transformed space using a second-order-accurate, optionally semi-Lagrangian or Eulerian, nonoscillatory forward-in-time (NFT) approach, broadly documented in the literature (cf. Reference [14] for a recent review; alternatively see Reference [12] in the same issue for a brief summary). Here we employ the flux-form Eulerian, semi-implicit version of the algorithm based on the monotone MPDATA transport scheme [15]. All prognostic equations in (2) are integrated along flow trajectories using the trapezoidal rule, treating all forcings on the rhs implicitly; the viscous and diffusive terms are computed to first-order accuracy, assuming $\nabla\cdot\tau^{n+1} = \nabla\cdot\tau^n + \mathcal{O}(\Delta t)$ (and similar for $\kappa\nabla^2\rho'$); see Section 3.5.4 in Reference [15]. Together with the curvilinearity of the coordinates, this leads to a complicated elliptic problem for pressure (see Appendix A in Reference [11] for the complete description) solved iteratively using the preconditioned generalized conjugate-residual approach—a non-symmetric Krylov-subspace solver [16].

3. THE QUASI-BIENNIAL OSCILLATION ANALOGUE

The laboratory experiment of Plumb and McEwan was conducted in a transparent cylindrical annulus (radii $a = 0.183$ m and $b = 0.3$ m) filled with density-stratified salty water to

a height of $z_{ab} = 0.43$ m. The lower boundary consisted of a thin rubber membrane which oscillated with a constant frequency ω_0 [5]. In our numerical simulation of their laboratory setup we assume an initially stagnant, viscous Boussinesq fluid forced by an oscillating lower boundary. The cylindrical setup of the laboratory tank is replaced with a zonally-periodic, rectangular[¶] computational domain consisting of $639 \times 38 \times 188$ grid intervals with $L_x = 2\pi(a+b)/2$, $L_y = b - a$, $L_z = 0.6$ m and impermeable boundaries. The lower boundary shape is specified as

$$z_s(x, y, t) = \varepsilon \sin\left(\frac{\pi}{L_y}\, y\right) \sin\left(\frac{2\pi s}{L_x}\, x\right) \sin(\omega_0 t) \tag{4}$$

with $s = 8$ and forcing amplitude $\varepsilon = 0.008$ m. The initial condition is assumed identical to the static ambient state with a buoyancy frequency $N = 1.88\,\mathrm{s}^{-1}$. The integration time was several hours with a time-step $\mathrm{d}t = 0.05$ s. The distance $L_z - z_{ab}$ is designated to an absorbing layer, which suppresses spurious wave reflection from the upper rigid lid, simulating an infinite water tank. In our 3D simulations we find, however, reflections from the upper boundary to be negligible in agreement with laboratory observations [5].

Starting from a zero background flow we observe symmetrical, upward propagating, standing gravity waves in the horizontal. After approximately 1–2 h (in agreement with laboratory observations [5])[‖] the wave field distorts. A single horizontal and a range of vertical wave numbers are observed in each phase of the zonal mean flow oscillation. The internal waves interfere with each other in the vertical, and spatial patterns of reinforcement and cancellation appear. Subsequently, the coherent wave structures break down, and locally zonal flow shear layers of critical magnitude form, giving rise to an apparent downward propagation of a mean zonal flow pattern which reverses sign in a periodic manner. Figure 1 shows time-height cross-sections of the zonal mean flow for two representative simulations. Table I summarizes the quantitative comparison between our simulations and the laboratory analogue of Plumb and McEwan. The table also shows results of the experiment repeated at the university of Kyoto [18] where the oscillating membrane was placed at the top of an annulus initiating an oscillation with an apparent upward propagation of the mean flow. In this case the correct physical lower boundary is a rigid lid and the upper boundary entering the transformation in (3) is given as

$$H(x, y, t) = H_0 - z_s(x, y, t) \tag{5}$$

Notable in the results of Table I is our inability to reproduce the precise period of the original Plumb and McEwan experiment; yet by doubling the frequency or the physical domain (viz. the horizontal wavelength) we obtain comparable periods. However, our numerical analogue of the Kyoto experiment setup compares favourably. In particular, the filmed time evolution of the experiment [18] agrees well with our numerical simulation. In all experiments the observed mean flow magnitude is consistent with predictions from linear theory of critical

[¶] A better comparability of simulated and laboratory results for larger annuli (see Table I) suggests that curvature effects (see Reference [17] for a discussion) may be worth investigating; we hope to address this in future.

[‖] We find that we can save substantial CPU time (without affecting the results) by forcing an initial oscillation with a background flow in the near-membrane layers. This mechanism has been used in all simulations summarized in Table I.

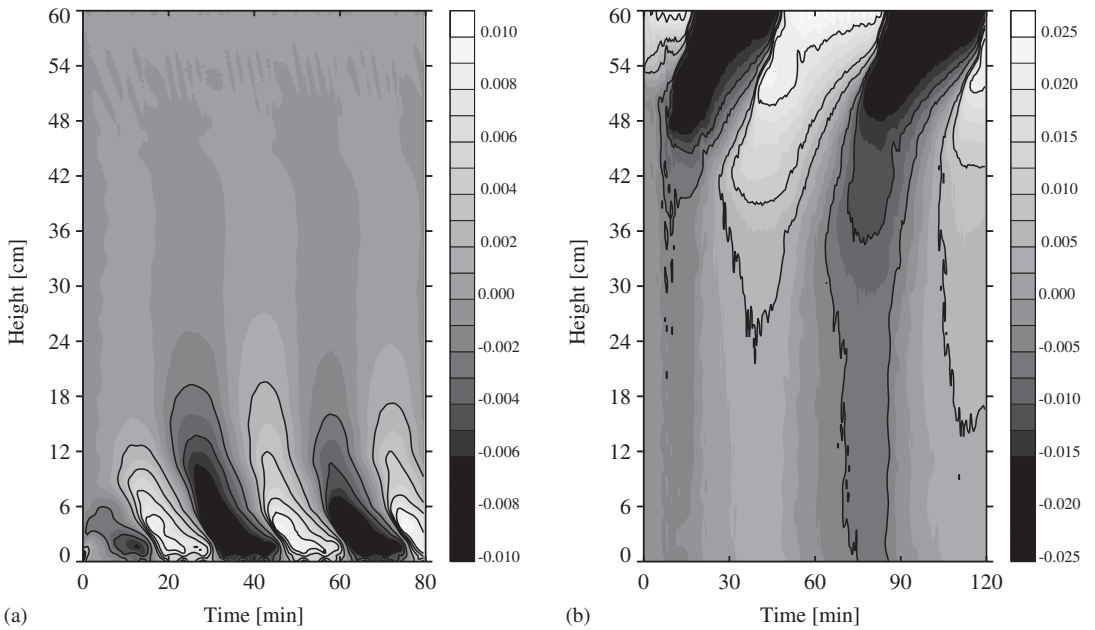

Figure 1. Time-height cross-sections of the zonal mean flow velocity at $y = L_y/2$ in our numerical simulations. Plate a shows the Plumb and McEwan numerical analogue [case (c) in Table I] and plate (b) shows our results for the Kyoto laboratory setup [case (d) in Table I]. Plate (a) compares with Figure 10 in Reference [5]. The units are in ms^{-1}.

Table I. Comparison of the zonal mean flow oscillations in the laboratory experiments [Lab] (Plumb and McEwan [P + E] and the university of Kyoto [Kyoto]) and in our numerical simulations [Num].

Description*	L_x [m]	L_y [m]	L_z [m]	ε [mm]	ω_0 [s^{-1}]	N [s^{-1}]	T_0 [min]	z_0 [m]	A_0 [ms^{-1}]
(a) Lab: P + E	1.52	0.117	0.43	8.0	0.43	1.88	82	0.2	0.0085
(b) Lab: Kyoto	3.14	0.2	0.6	11.0	0.40	1.60	76	—	—
(c) Num: P + E	1.52	0.117	0.6(0.43)	8.0	0.43	1.88	32	0.18	0.009
(d) Num: Kyoto	3.14	0.2	0.6	11.0	0.40	1.60	76	0.3	0.023
(e) Num: P + E	3.14	0.2	0.6(0.43)	8.0	0.43	1.88	100	0.4	0.022
(f) Num: P + E	1.52	0.117	0.6(0.43)	8.0	0.86	1.88	106	0.4	0.025

T_0, z_0, and A_0 symbolize the period, the vertical extent, and the observed maximum mean-flow speed of the zonal mean zonal flow oscillation, respectively, for the given domain (viz. wave length), forcing frequency ω_0, forcing amplitude ε, and stratification N.

* The value for T_0 in the Kyoto setup is deduced from the movie found in Reference [18]; z_0 and A_0 are not given. The value for N in the P + E setup is obtained from the derived values of Figure 10 in Reference [5], $T_0 = 476$, $d_0 = 0.17$, and their formulas 4.10–4.12. All other values are taken as stated in the cited references.

levels (i.e. postulated by the singularity of the Taylor–Goldstein equation [19, pp. 320–324])

$$U_{\mathrm{crit}} = \frac{\omega_0}{(2\pi s/L_x)} \tag{6}$$

and we find that the period of the oscillation is sensitive to U_{crit}.

4. REMARKS

We find numerical evidence that the periodically reversing mean flow pattern in the laboratory analogue is driven by internal wave–wave mean flow interactions with a non-zero momentum flux divergence primarily resulting from vertical wave interference, subsequent wave momentum flux changes and locally, critical layer wave attenuation enhanced by wave breaking.

A comprehensive analysis of the gathered numerical data underline our conclusions and reveal a different interpretation of the oscillation mechanism than that described in Reference [7]. This is discussed in Reference [20] together with a detailed account of the numerical and parametric sensitivities and a discussion of the theoretical and practical implications on the atmospheric QBO.

REFERENCES

1. Baldwin MP, Gray LJ, Dunkerton TJ, Hamilton K, Haynes PH, Randel WJ, Holton JR, Alexander MJ, Hirota I, Horinouchi T, Jones DBA, Kinnersley JS, Marquardt C, Sato K, Takahashi M. The quasi-biennial oscillation. *Reviews of Geophysics* 2001; **39**(2):179–229.
2. Lindzen RS, Holton JR. A theory of the quasi-biennial oscillation. *Journal of the Atmospheric Sciences* 1968; **25**:1095–1107.
3. Holton JR, Lindzen RS. An updated theory for the quasi-biennial cycle of the tropical stratosphere. *Journal of the Atmospheric Sciences* 1972; **29**:1076–1079.
4. Eliassen A, Palm E. On the transfer of energy in stationary mountain waves. *Geofysiske Publikasjoner* 1961; **22**:1–23.
5. Plumb RA, McEwan D. The instability of a forced standing wave in a viscous stratified fluid: a laboratory analogue of the quasi-biennial oscillation. *Journal of the Atmospheric Sciences* 1978; **35**:1827–1839.
6. Dunkerton TJ. Wave transience in a compressible atmosphere. Part II: Transient equatorial waves in the quasi-biennial oscillation. *Journal of the Atmospheric Sciences* 1981; **38**:298–307.
7. Plumb RA. The interaction of two internal waves with the mean flow: implications for the theory of the quasi-biennial oscillation. *Journal of the Atmospheric Sciences* 1977; **34**:1847–1858.
8. McIntyre ME. On global-scale atmospheric circulations. In *Perspectives in Fluid Dynamics: A Collective Introduction to Current Research*, Batchelor GK, Moffatt HK, Worster MG (eds). Cambridge University Press: Cambridge, 2003; 557–624.
9. Galmiche M, Thual O, Bonneton P. Wave/wave interaction producing horizontal mean flows in stably stratified fluids. *Dynamics of Atmospheres and Oceans* 2000; **31**:193–207.
10. Gill A. *Atmosphere-Ocean Dynamics*. Academic Press: London, 1982.
11. Prusa JM, Smolarkiewicz PK. An all-scale anelastic model for geophysical flows: dynamic grid deformation. *Journal of Computational Physics* 2003; **190**:601–622.
12. Smolarkiewicz PK, Prusa JM. Toward mesh adaptivity for geophysical turbulence. *International Journal for Numerical Methods in Fluids* 2004; *ibid.*
13. Wedi NP, Smolarkiewicz PK. Extending Gal–Chen and Somerville terrain-following coordinate transformation on time-dependent curvilinear boundaries. *Journal of Computational Physics* 2004; **193**:1–20.
14. Smolarkiewicz PK, Prusa JM. Forward-in-time differencing for fluids: simulation of geophysical turbulence. In *Turbulent Flow Computations*, Drikakis D, Guertz BJ (eds). Kluwer Academic Publishers: Dordrecht, 2002; 207–240.
15. Smolarkiewicz PK, Margolin LG. MPDATA: a finite difference solver for geophysical flows. *Journal of Computational Physics* 1998; **140**:459–480.
16. Smolarkiewicz PK, Margolin LG. Variational methods for elliptic problems in fluid models. *Proceedings of the ECMWF Workshop on Developments in Numerical Methods for Very High Resolution Global Models*, 5–7 June 2000, ECMWF, Reading, U.K., 2000; 137–159.
17. Read PL, Lewis SR, Hide R. Laboratory and numerical studies of baroclinic waves in an internally heated rotating fluid annulus: a case of wave/vortex duality? *Journal of Fluid Mechanics* 1997; **337**:155–191.
18. Observing Reversing Currents. http://www.gfd-dennou.org/library/gfd_exp/exp_e/exp/bo/1/app.htm (10 January 2004).
19. Drazin PG, Reid WH. *Hydrodynamic Stability*. Cambridge University Press: Cambridge, 1981.
20. Wedi NP. Time-dependent boundaries in numerical models. *Ph.D. Thesis*, Ludwig-Maximilians-Universität München, 2004.

